10.24425/acs.2019.127526

Archives of Control Sciences
Volume 29(LXV), 2019
No. 1, *pages 111–132*

Preview Control applied for humanoid robot motion generation

MAKSYMILIAN SZUMOWSKI, MAGDALENA SYLWIA ŻURAWSKA and TERESA ZIELIŃSKA

This paper presents a concept of humanoid robot motion generation using the dedicated simplified dynamic model of the robot (Extended Cart-Table model). Humanoid robot gait with equal steps length is considered. Motion pattern is obtained here with use of Preview Control method. Motion trajectories are first obtained in simulations (off-line) and then they are verified on a test-bed. Tests performed using the real robot confirmed the correctness of the method. Robot completed a set of steps without losing its balance.

Key words: motion generation, humanoid robot, Preview Control, Extended Cart-Table model, off-line method

1. Introduction

Legged locomotion prevails on wheeled locomotion in situations where robot must traverse on unpredictable terrains (e.g. destroyed buildings or uneven terrain). However humanoid robot motion generation is a laborious issue with comparison to the stability of e.g. wheeled robots. A lot of research have been done on humanoids' motion synthesis so far (i.e. [1, 2, 11, 13]).

Legged locomotion is more difficult in synthesis because it requires precise footstep placement with proper posture shaping to avoid loosing robot's balance. Wheeled mobile robot is intrinsically statically stable, while in the case of humanoid robot, the dynamic stability must be considered (e.g. with accordance to the well known stability criterion – Zero Moment Point Criterion, ZMP [17]). The main concept behind mentioned criterion is the idea of balancing forces and moments with respect to a certain point – Zero Moment Point.

In the dynamic computation of the humanoid robots, a common practice is to substitute highly complicated dynamic structures of those robots by simplified

All the Authors are with Warsaw University of Technology, The Faculty of Power and Aeronautical Engineering, Warsaw, Nowowiejska 24 Str, Poland

This work was supported by "Diamond Grant" founded by Polish Ministry of Science and Higher Education (no 0072/DIA/2014/43), *Development and testing of a method for dynamic gait synthesis with the use of a new-design robot*.

Received 15.01.2019. Revised 01.03.2019

models (e.g. [4,8,9]). It is done due to high cost of dynamics computations. Such action allows speeding up the computations (computation with use of complicated kinematic structures are time-consuming and tremendous) but at the expense of simplifications – simplified models don't take the full dynamics [14].

The proper trajectory planning for active joints is crucial in humanoid robot motion synthesis and Preview Control [5] or Model Predictive Control [16] methods are here advantageous (e.g. [3,10,12]). Motion generation often applies those methods with state equations representing the inverted pendulum dynamics. The body is reduced here to a single point mass (CoM) on a massless link [4]. In Preview Control the primary objective is to obtain the CoM motion trajectory resembling the trajectory of human CoM. Using the simplified model of a humanoid, the predictive controller generates the dynamic trajectory of the center of mass, and the control system of a real robot is tracking it in a best possible way.

ZMP criterion can be applied in both: – control methods with very complex kinematic structures of humanoid robot, and – control methods with simplified dynamic models.

The predictive methods not only use the information from the current time instant but also the prediction about future data. With predictive approach the regulator reacts in advance to the changes of reference trajectories adjusting properly the depended variables.

Motion generation methods are on-line [6] or off-line [15] type. Because of time factor in on-line methods the simplified robot's models can only be considered (e.g. [4]). In off-line methods the gait is first generated using simulation approaches, and next is implemented and tested in the hardware.

The goal of this paper is to deliver the motion generation method based on the idea of off-line predictive control. The new simplified dynamic model of the robot is introduced. The method was verified on the robot prototype designed by the authors.

The main contribution of this paper lies both in theoretical and hardware part. The theoretical background of this paper is based on [3, 5], however ideas presented in above articles are broaden. The simplified model presented in [3] is the Cart-Table Model. In case of the available hardware, the model had to be extended. The extension was done by the authors and is described in the first part of the article. This implies the necessity to adapt the theoretical derivation of Preview Control formulas presented in [5] to the extended model. Moreover, the Zero Moment Point Concept presented in [3] was also adapted to the extended model. Authors also rezognize the need of universal control scheme and introduces the modularity concept (that is described in further part of the paper). The correctness of method described in paper cited above was proven only using simulations. So the novelty of this paper with comparison to works described in [3] is also the hardware implementation.

The structure of this paper is arranged in a following way. First, the simplified dynamic model of the robot is described. We consider here the robot prototype developed by us. Next, the Preview Control scheme for mentioned model is derived. After that, the general concept of motion generation method is described. The presentation is followed by the specific example and the implementation on the real humanoid robot is presented. Conclusions and plans for the future works closes the article.

2. Simplified dynamic model – Extended Cart-Table

We consider the kinematic structure of a humanoid robot depicted in Fig. 1. The robot has 8 degrees of freedom: 3 DoFs for each leg and one for each upper extremity. We consider the planar robot. We assume that the arms are affixed to the body, along the torso, by those reducing the system to 6 DOF's planar robot. Fixing the DoFs from the upper extremities allows us to use the simplified model as it is presented below.

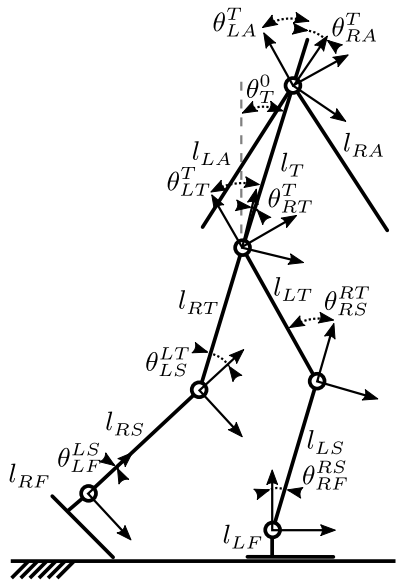

Figure 1: Kinematic structure of the robot considered in presented research

Following the assumption of predictive control applied for humanoids, the complex model of a humanoid robot is simplified to the model of Cart-Table (Fig. 2). However we expanded the Cart-Table model derived from [3] with the stabilizer part (which is an integral element of our test bed). Schematic diagram

of our concept together with parameters describing our model are shown in Fig. 2 together with the sketch of the real robot.

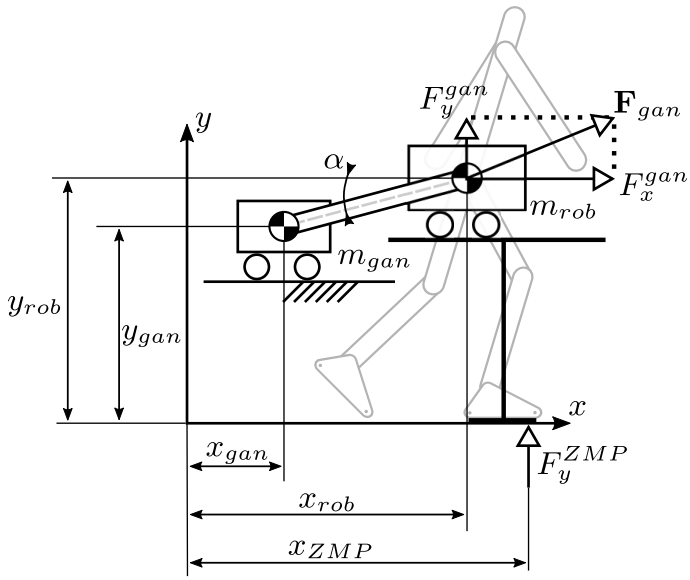

Figure 2: Schematic diagram of the Extended Cart Table model together with the reference to the real robot

The Center of Mass of the humanoid robot (m_{rob}) is denoted by $[x_{rob}, y_{rob}]^T$, while the Center of Mass of the gantry (m_{gan}) is – $[x_{gan}, y_{gan}]^T$. In our example the y_{rob} and y_{gan} coordinates (vertical) are constant. Gantry mass is not negligible, so it is considered in the simplified model. We designed our own model which includes the Cart-Table system and the gantry (part of robot motion stabilizer). Due to this extension, all necessary parameters are considered.

Reaction forces coming from the foot of the robot (and therefore the reaction forces coming from the simplified model) are described with use of the idea of Zero Moment Point [17]. For further calculation, only the vertical component (along y axis) of the reaction force will be considered and denoted by F_y^{ZMP}. The point, where F_y^{ZMP} is applied is the x_{ZMP} coordinate.

3. ZMP preview control for Extended Cart Table model

In our gait generation method, the set-point is the Center of Mass (CoM) location – we assumed that the Center of Mass of the robot remains on a constant level during the whole movement. The tracked value (given) is the location of the Zero Moment Point (ZMP). Describing the equilibrium of sum of moments

in the system depicted in the Fig. 2 around z axis, we have:

$$0 = x_{ZMP}F_y^{ZMP} + y_{rob}m_{rob}\ddot{x}_{rob} + gm_{rob}x_{rob} + y_{rob}F_x^{gan} + x_{rob}F_y^{gan}, \tag{1}$$

where:

$$\mathbf{F}_{gan} = [F_x^{gan}\ F_y^{gan}]^{\mathrm{T}} = [|\mathbf{F}_{gan}| \cdot \cos(\alpha), \qquad |\mathbf{F}_{gan}| \cdot \sin(\alpha)]^{\mathrm{T}}. \tag{2}$$

Substituting F_x^{gan} and F_y^{gan} into Eq. (2):

$$0 = x_{ZMP}F_y^{ZMP} + y_{rob}m_{rob}\ddot{x}_{rob} + gm_{rob}x_{rob} + y_{rob}|\mathbf{F}_{gan}|\cos(\alpha) + x_{rob}|\mathbf{F}_{gan}|\sin(\alpha), \tag{3}$$

where the $\mathbf{F}_{gan}$ is the force applied at point $[x_{rob}, y_{rob}]^{\mathrm{T}}$ coming from the gantry.

We denoted the angle between the horizontal axis and the line designated by points of the beginning and the end of the connector (those points are axes of rotation) as α. Because of the gantry construction, it is possible do attach the humanoid robot to the stabilizer in such way, that the connector between the gantry and the robot is set horizontally. Setting the connector horizontally implies the assumption that α is close to zero. Therefore $F_y^{gan} = 0$ and $F_x^{gan} = |\mathbf{F}_{gan}|$ and $|\mathbf{F}_{gan}| = m_{gan}\ddot{x}_{gan}$.

Because the connector is a rigid body, the distance between between x_{gan} and x_{rob} points is fixed. Therefore accelerations of those points are equal: $\ddot{x}_{gan} = \ddot{x}_{rob}$.

The Eq. (3) can be simplified to:

$$0 = x_{ZMP}F_y^{ZMP} + y_{rob}(m_{rob} + m_{gan})\ddot{x}_{rob} + gm_{rob}x_{rob}\,. \tag{4}$$

The only unknown value in the Eq. (4) is the reaction force in the Zero Moment Point (y component). Maintaining the assumption of $\alpha = 0$, we can state the force equilibrium along y axis:

$$0 = F_y^{ZMP} + gm_{rob}. \tag{5}$$

Substituting Eq. (5) into Eq. (4) we obtain:

$$x_{ZMP} = x_{rob} + \frac{y_{rob}}{g}\ddot{x}_{rob}\left(\frac{m_{gan}}{m_{rob}} + 1\right), \tag{6}$$

where x_{ZMP} is the horizontal coordinate of the Zero Moment Point obtained for the whole gait, that means for both: the single and the double support phases.

4. Gait generation method

Authors recognized the need of the universal control scheme for humanoid robot motion generation. The idea behind is to have one general concept for different movement scenarios, eg. gait with constant/variable steps length, manipulation/uplifting of objects or kicking the ball (action necessary for competition like RoboCup Soccer [20]). Authors standardized inputs and outputs to each block of the control scheme. In view of this fact, nevertheless the movement type, the signals flow between each stage of the algorithm, will be the same. This is the modularity concept – blocks with different concepts can be chained together.

The gait generation method presented in this article consists of 4 main stages: task description, step planning, generation of position of centre of mass and inverse kinematic solution. Each stage provides data relevant to the subsequent stages. In Fig. 3 we have presented block diagram of proposed method. In the further part of the article, each stage is described.

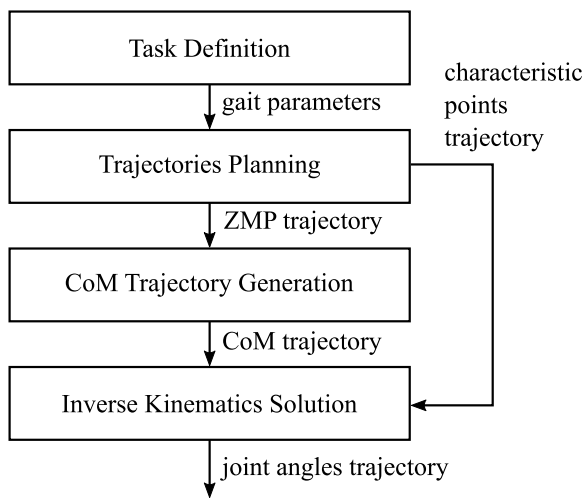

Figure 3: Block diagram of data flow in proposed method

In the schema presented in Fig. 3 the modularity concept can be seen. There are four blocks, each block presents different stage of the algorithm. In the view of this fact, it is possible to check different movement types (defined in "Task definition" block), holding the same trajectories planning and inverse kinematics algorithms.

4.1. Task definition (stage 1)

In stage 1, we define the gait characteristics that we want to obtain. Relevant parameters are determined (height of the centre of mass, duration of the gait cycle,

number of gait cycles, proportion of gait phases in gait cycle, sampling time). Moreover the data defining the robot's kinematic model and steps length data are loaded. In this paper we have assumed that the centre of mass of the robot will moving holding a constant height. In stage 1 defined parameters are verified. It is checked whether the gait with given parameters is feasible and the step length is such that it fits the leg workspace. Feasibility is concluded considering the limitations of the mechanical and control systems.

4.2. Trajectories planning (stage 2)

In this stage the reference trajectories of robot joints are designed – that the steps concluded in stage 1 will be achieved. First the step placement areas are selected. In this work, we assume, that the steps' lengths are equal. Information declared in stage 1 are used to design the areas, where robot can put it's feet. Those areas are defined as a circle with given center and radius. The "trajectory planning block" is fed with this data, expressed in the reference frame attached to the torso of the robot. This concept is valid for both the 3D and the planar robot – robot that performs movements only in sagittal plane. It should be noted, that in the case of planar robot, the area of foot placement is degenerated to a line segment.

Zero Moment Point ([17]) is widely known and commonly used method for evaluating the postural stability of the robot. According to this criterion, the posture of the robot is stable, when the Zero Moment Point is within the robot's footsole (for single support phase) or within the area established by two footprints (double support phase). In our case (planar robot with – movements only in sagittal plane), lateral component of ZMP is not present – robot does not perform side movements). Therefore the ZMP in a given time instant must be located within the line segment bounded by two extremities of the foot (or the feet) – toes and heels.

Basing on information about the foot placement the reference trajectory of ZMP (both for single and double support phases) is produced. Taking into account the modelling simplifications and all possible disturbances, it is desirable to maintain the ZMP possibly close to the center of the mentioned line segment. Therefore, authors assumed that ZMP coordinate for single support phase is described by following equation:

$$x_{ZMP}^{ref}(i) = \frac{x_a(i) - x_b(i)}{2}, \tag{7}$$

where i means i-th moment of time, x_{ZMP}^{ref} is the reference trajectory of ZMP, x_a is one of two foot's endpoints (eg. point located in toes), and x_b is a second endpoint (eg. point located in a heel). For double support phase, we use similar formula, but points (x_a and x_b) concern appropriately left plus right foot.

Having information about planned steps, trajectories of ankle joints are obtained (characteristic points) as a polynomials of 3rd (along y axis) Eq. (9) and 5th order (along x axis) Eq. (8). The foot orientation in the transfer phase is also obtained Eq. 10).

$$x_{ankle} = a_{x5}t^5 + a_{x4}t^4 + a_{x3}t^3 + a_{x2}t^2 + a_{x1}t + a_{x0} \qquad \text{for} \quad t_{start} \leqslant t \leqslant t_{end}, \tag{8}$$

$$y_{ankle} = \begin{cases} a_{y3.1}t^3 + a_{y2.1}t^2 + a_{y1.1}t + a_{y0.1} & \text{for} \quad t_{start} \leqslant t \leqslant 0.5t_{end}, \\ a_{y3.2}t^3 + a_{y2.2}t^2 + a_{y1.2}t + a_{y0.2} & \text{for} \quad 0.5t_{end} < t \leqslant t_{end}, \end{cases} \tag{9}$$

$$\theta_{ankle} = 0 \qquad \text{for} \quad t_{start} \leqslant t \leqslant t_{end}. \tag{10}$$

Evaluating the unknown parameters a_x, a_y in Eq. (8), (9) we consider the boundary conditions for positions, velocities and accelerations on the ends of defined ranges. Ankle trajectories and points – boundary conditions are depicted in Fig. 4 and in Fig. 5. Boundary conditions (points) are marked with use of "X"

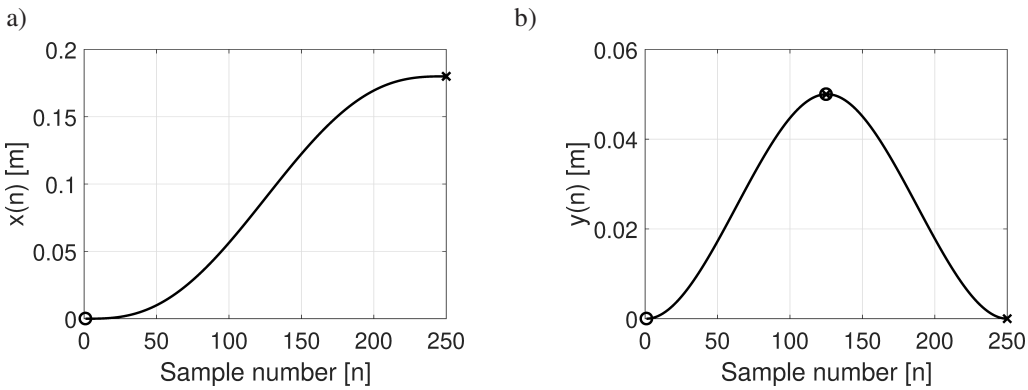

Figure 4: Ankle trajectory as a function of sample's number: a) x coordinate, b) y coordinate. Boundary conditions (start and end) for each polynomial are marked as "O" and "X"

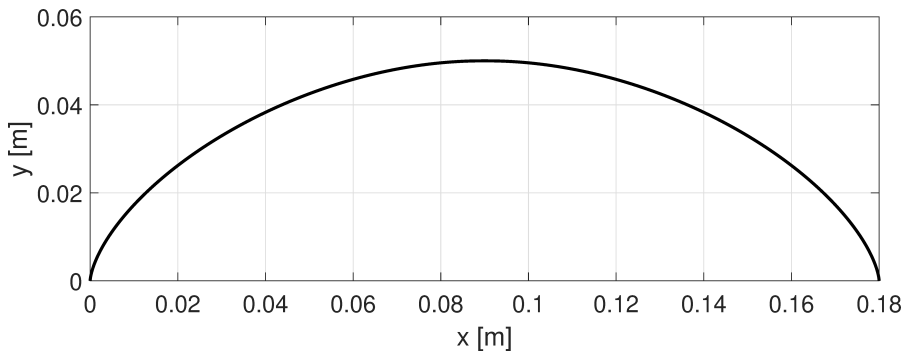

Figure 5: Ankle trajectory $y(x)$

sign and "O" sign. For the a_y in Eq. (9) we additionally consider the middle of the range (twice – because y coordinate is the same in the end of the first part of the trajectory and in the beginning of the second part of the trajectory, as it is shown in Fig. 4b).

4.3. CoM trajectory generation (stage 3)

All data listed in the previous section (ZMP reference trajectory, trajectories of characteristic points and foot orientation) are necessary for evaluation robot's centre of mass trajectory. The Preview Control scheme allows us to obtain the CoM trajectory basing on the ZMP trajectory.

The reference value is then reference position of ZMP (calculated with formula (7)), while the followed (by the robot) value is the ZMP output from the model (a realistic, predicted trajectory). In our method we adopt the Preview Control prediction method (as in the article [3]), with the difference that in our case we use the extended Cart-Table model [15].

System with Preview Control regulator is shown in Fig. 6. Input to the system is ZMP trajectory x_{zmp}^{zad} while output is x_{zmp} – obtained trajectory of ZMP, considering the robot model.

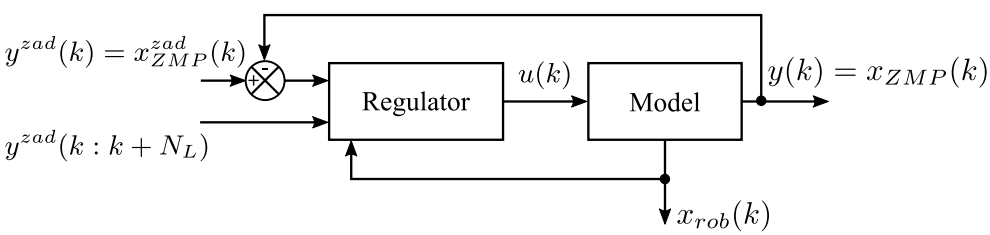

Figure 6: Preview Control concept applied for trajectory generation

Model used in system from Fig. 6 is described in form of state-space equation:

$$\frac{\mathrm{d}}{\mathrm{d}t}\begin{bmatrix} x_1 \\ x_2 \\ x_3 \end{bmatrix} = \begin{bmatrix} 0 & 1 & 0 \\ 0 & 0 & 1 \\ 0 & 0 & 0 \end{bmatrix}\begin{bmatrix} x_1 \\ x_2 \\ x_3 \end{bmatrix} + \begin{bmatrix} 0 \\ 0 \\ 1 \end{bmatrix} u, \tag{11}$$

where x_1, x_2, x_3 are the state variables: x_1 is the location of the center of mass of the robot (x_{rob}), x_2 is the velocity of CoM and x_3 is the acceleration – along x axis:

$$\begin{bmatrix} x_1 \\ x_2 \\ x_3 \end{bmatrix} = \begin{bmatrix} x_{rob} \\ \dot{x}_{rob} \\ \ddot{x}_{rob} \end{bmatrix} \tag{12}$$

and using Eq. (6) we define the output from the system as:

$$y = x_{ZMP} = \left[1 \quad 0 \quad \frac{h_{rob}}{g}\left(1 + \frac{m_{gan}}{m_{rob}}\right)\right][x_1 \quad x_2 \quad x_3]^{\mathrm{T}}. \tag{13}$$

The variable u has been defined as a third derivative of x_1–x coordinate of the point mass (as it is done in [4]):

$$u = \dot{x}_3 = \dddot{x}_{rob}. \tag{14}$$

To use the Preview Control scheme, Eq. (11)–(14) should be discretized. The state equations in discrete form (T – constant sampling time):

$$\mathbf{x}(k+1) = \mathbf{A}\mathbf{x}(k) + \mathbf{B}u(k), \tag{15}$$

$$y(k) = \mathbf{C}\mathbf{x}(k), \tag{16}$$

where:

$$\mathbf{A} = e^{\mathbf{A}_{con}T} = \begin{bmatrix} 1 & T & \frac{T^2}{2} \\ 0 & 1 & T \\ 0 & 0 & 1 \end{bmatrix}, \qquad \mathbf{B} = \int_0^T e^{\mathbf{A}_{con}s}\,\mathrm{d}s\,\mathbf{B}_{con} = \begin{bmatrix} \frac{T^3}{6} \\ \frac{T^2}{2} \\ T \end{bmatrix},$$

$$\mathbf{C} = \begin{bmatrix} 1 & 0 & \frac{h_{rob}}{g}\left(1 + \frac{m_{gan}}{m_{rob}}\right) \end{bmatrix}$$

and:

$$\mathbf{A}_{con} = \begin{bmatrix} 0 & 1 & 0 \\ 0 & 0 & 1 \\ 0 & 0 & 0 \end{bmatrix}, \qquad \mathbf{B}_{con} = \begin{bmatrix} 0 \\ 0 \\ 1 \end{bmatrix}.$$

Quality criterion, taking into account reference trajectory of the Zero Moment Point $x^{ref}(k)$ (based on [5]):

$$J = \sum_{i=k}^{\infty} \left\{ Q_e e(i)^2 + \Delta\mathbf{x}^{\mathrm{T}}(i)\mathbf{Q}_x\Delta\mathbf{x}(i) + R\Delta u^2(i) \right\}, \tag{17}$$

where the error is defined as:

$$e(i) \equiv x_{ZMP}^{zad}(i) - x_{ZMP}(i). \tag{18}$$

In equation (17) Q_e, $R > 0$ while $\mathbf{Q}_x$ is positive-definite symmetrical diagonal matrix 3×3 with fixed positive coefficients. In this case, we have a vector of state variables and input defined incrementally:

$$\Delta\mathbf{x}(k) \equiv \mathbf{x}(k) - \mathbf{x}(k-1), \tag{19}$$

$$\Delta u(k) \equiv u(k) - u(k-1). \tag{20}$$

Predictive method allows to forecast (at each step) the reference trajectory of ZMP for N_L steps ahead. In this work, we have adapted regulator from work [3] minimizing the quality index (17) and expressed by:

$$u(k) = -G_i \sum_{i=0}^{k} e(k) - \mathbf{G}_x \mathbf{x}(k) - \sum_{j=1}^{N_L} \mathbf{G}_p(j) x^{zad}(k+j), \tag{21}$$

where parameters G_i, $\mathbf{G}_x$ and $\mathbf{G}_p(j)$ have been computed from parameters Q_e, $\mathbf{Q}_x$ and matrices $\mathbf{A}$, $\mathbf{B}$ and $\mathbf{C}$.

To compute parameters G_i, $\mathbf{G}_x$ and $\mathbf{G}_p(j)$ the following formulas are used [5]:

$$\widetilde{\mathbf{G}}_i = [R + \widetilde{\mathbf{B}}^{\mathrm{T}} \widetilde{\mathbf{K}} \widetilde{\mathbf{B}}]^{-1} \widetilde{\mathbf{B}}^{\mathrm{T}} \widetilde{\mathbf{K}} \widetilde{\mathbf{B}}, \tag{22}$$

$$\widetilde{\mathbf{G}}_x = [R + \widetilde{\mathbf{B}}^{\mathrm{T}} \widetilde{\mathbf{K}} \widetilde{\mathbf{B}}]^{-1} \widetilde{\mathbf{B}}^{\mathrm{T}} \widetilde{\mathbf{K}} \widetilde{\mathbf{F}}, \tag{23}$$

$$\widetilde{\mathbf{G}}_p(1) = -\widetilde{\mathbf{G}}_i, \tag{24}$$

$$\widetilde{\mathbf{G}}_p(l) = [R + \widetilde{\mathbf{B}}^{\mathrm{T}} \widetilde{\mathbf{K}} \widetilde{\mathbf{B}}]^{-1} \widetilde{\mathbf{B}}^{\mathrm{T}} \widetilde{\mathbf{X}}(l-1), \qquad l = 2, \ldots, N_L. \tag{25}$$

In above formulas we have used: $\widetilde{\mathbf{A}}$, $\widetilde{\mathbf{B}}$, $\widetilde{\mathbf{I}}$, $\widetilde{\mathbf{F}}$, $\widetilde{\mathbf{Q}}$, $\widetilde{\mathbf{K}}$ and $\widetilde{\mathbf{X}}$ that are defined accordingly:

$$\widetilde{\mathbf{B}} = \begin{bmatrix} \mathbf{CB} \\ \mathbf{B} \end{bmatrix}, \tag{26}$$

$$\widetilde{\mathbf{I}} = \begin{bmatrix} I_p \\ \mathbf{0}_{3\times 1} \end{bmatrix} = \begin{bmatrix} 1 \\ \mathbf{0}_{3\times 1} \end{bmatrix}, \tag{27}$$

where I_p denotes $p \times p$ unit matrix (in our case, where $p = 1$ it is scalar 1):

$$\widetilde{\mathbf{F}} = \begin{bmatrix} \mathbf{CA} \\ \mathbf{A} \end{bmatrix}, \tag{28}$$

$$\widetilde{\mathbf{Q}} = \begin{bmatrix} Q_e & \mathbf{0}_{1\times 3} \\ \mathbf{0}_{3\times 1} & \mathbf{Q}_x \end{bmatrix}, \tag{29}$$

$$\widetilde{\mathbf{A}} = \begin{bmatrix} \widetilde{\mathbf{I}} & \widetilde{\mathbf{F}} \end{bmatrix} \tag{30}$$

and where matrix $\widetilde{\mathbf{K}}$ is the non-negative definite solution of the algebraic Riccati equation (equation is in steady-state, time subscripts are removed from equation):

$$\widetilde{\mathbf{K}} = \widetilde{\mathbf{A}}^{\mathrm{T}} \widetilde{\mathbf{K}} \widetilde{\mathbf{A}} - \widetilde{\mathbf{A}}^{\mathrm{T}} \widetilde{\mathbf{K}} \widetilde{\mathbf{B}} [R + \widetilde{\mathbf{B}}^{\mathrm{T}} \widetilde{\mathbf{K}} \widetilde{\mathbf{B}}]^{-1} \widetilde{\mathbf{B}}^{\mathrm{T}} \widetilde{\mathbf{K}} \widetilde{\mathbf{A}} + \widetilde{\mathbf{Q}}. \tag{31}$$

Matrices $\widetilde{\mathbf{X}}(l)$ are given by:

$$\widetilde{\mathbf{X}}(1) = -\widetilde{\mathbf{A}}_c^{\mathrm{T}}\widetilde{\mathbf{K}}\widetilde{\mathbf{I}}, \tag{32}$$

$$\widetilde{\mathbf{X}}(l) = -\widetilde{\mathbf{A}}_c^{\mathrm{T}}\widetilde{\mathbf{X}}(l-1), \qquad l = 2, \ldots, N_L, \tag{33}$$

where $\widetilde{\mathbf{A}}_c$ is the closed loop matrix:

$$\widetilde{\mathbf{A}}_c = \widetilde{\mathbf{A}} - \widetilde{\mathbf{B}}[R + \widetilde{\mathbf{B}}^{\mathrm{T}}\widetilde{\mathbf{K}}\widetilde{\mathbf{B}}]^{-1}\widetilde{\mathbf{B}}^{\mathrm{T}}\widetilde{\mathbf{K}}\widetilde{\mathbf{A}}. \tag{34}$$

4.4. Inverse kinematics problem (stage 4)

Having information about the trajectory of the robot's centre of mass (obtained in stage 3 of the algorithm using simplified model), as well as the trajectories of characteristic points, we solve the inverse kinematic problem for the overall system, that is for the actual robot's kinematic scheme.

On the basis on the centre of mass trajectory and on the information about the characteristic points position, the inverse kinematic problem is solved. The result are trajectories for all joint angles:

$$\theta = \left[\theta_{RA}^T \;\; \theta_{LA}^T \;\; \theta_{RT}^T \;\; \theta_{LT}^T \;\; \theta_{RS}^{RT} \;\; \theta_{LS}^{LT} \;\; \theta_{RF}^{RS} \;\; \theta_{LF}^{LS}\right], \tag{35}$$

where θ_{RA}^T and θ_{LA}^T are equal zero.

5. Trajectory generation in simulations

5.1. Task definition (stage 1)

First stage of our algorithm is the definition of all necessary parameters for the task which we consider. It should be noted that parameters defined here are specific for the robot and the gait.

In our experiment robot performs 5 gait cycles lasting 1000 samples each (one sample takes 1 ms). Step length is 0.1 8m. We have assumed that double support phases and single support phases takes $\frac{1}{4}$ time of the whole gait cycle time. In Table 1 we have presented parameters that describe the generated gait.

The gait begins when robot is standing upright, with feet parallel to each other. Last movement (from defined by user set of steps) is performed so that in the last phase feet are in the same relative position as at the beginning – upright posture, feet parallel.

The gait defined above should be performed using a biped robot with 6 degrees of freedom (3 DoFs for each leg). Considered is a planar robot – all segments of the robot move only in sagittal plane.

Table 1: Gait parameters used in this work

Parameter	Value	Parameter	Value
Height of CoM	0.237 m	Number of gait cycles	5
Duration of one gait cycle	1000 samples	Sampling time	1 ms
Step length	0.1 8m	Duration of gait cycle	1 s
Percentage of single support phase	$2\times25\%$	Percentage of double support phase	$2\times25\%$

The kinematic structure of the robot is presented in Fig. 1 (the beginning of this paper). Segments' lengths and segments' masses are shown in the Table 2.

Table 2: Dimensions

Segment	Mass	Value [kg]	Length	Value [mm]
Shank	m_{LS}, m_{RS}	0.192	l_{LS}, l_{RS}	12.3
Trunk	m_T	0.696	l_T	14.4
Upper limb	m_{LA}, m_{RA}	0.091	l_{LA}, l_{RA}	11.0
Thigh	m_{LT}, m_{RT}	0.241	l_{LT}, l_{RT}	12.25
Foot	m_{LF}, m_{RF}	0.149	l_{LF}, l_{RF}	7.2
Support	m_{gan}	1.1	l_S	30.0
Robot CoM	m_{rob}	2.042	h_{rob}	24.5

5.2. Trajectories planning (stage 2)

Stage 2 provides the information about Zero Moment Point trajectory. In Fig. 7 reference ZMP trajectory (according to Eq. (7)) – ZMP Ref Trajectory and obtained ZMP trajectory are presented. The section where the ZMP trajectory must be located to ensure the stability of the robot is defined considering the frontal and rear edges of the feet (projected to the plane) – also shown in Fig. 7.

Fig. 7 illustrates how the obtained ZMP trajectory is located with respect to boundaries (front and rear points of the feet). If the location of the ZMP is within those boundaries, we conclude, that the posture of the robot is stable. Horizontal axis is the time line (number of sample), while vertical axis shows the distance from the beginning of the walk (we assumed that gait starts in $[0,0]$ point).

Obtained trajectory (bold line) is very close to the reference trajectory (grey line), and remains well in the limits. It means that the posture of the robot during

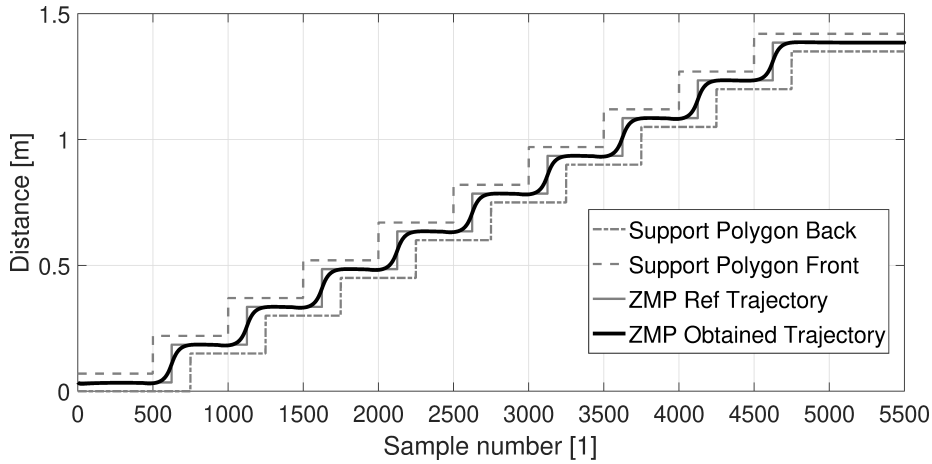

Figure 7: Comparison of the obtained trajectory of ZMP with reference trajectory. The ends (front and back) of foot supports are also shown

the entire gait is stable. Obtained ZMP trajectory can be then used to generate trajectory of centre of mass of the whole robot.

5.3. CoM trajectory generation (stage 3)

The Center of Mass (of the whole biped robot) trajectory is evaluated using the previous stages data (the ZMP trajectory and the simplified robot model). The outputs from the third stage (CoM trajectory) is presented in Fig. 8. As it can be seen, the trajectory is smooth, so the gait should be performed without disturbing displacements.

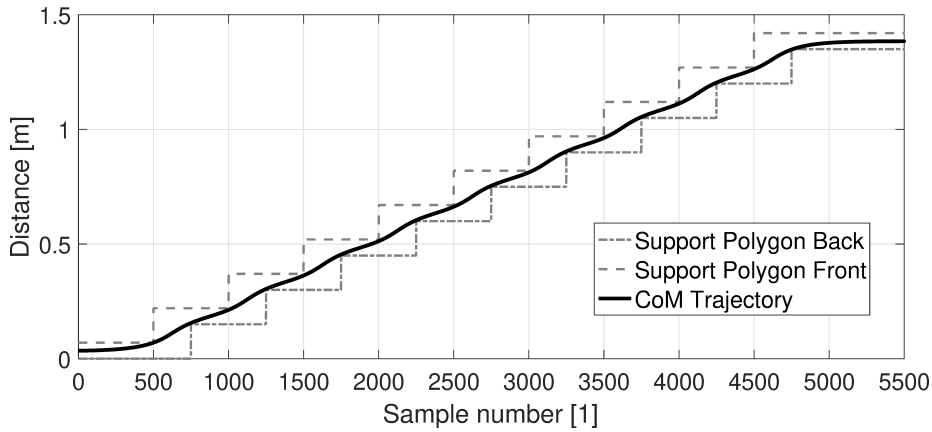

Figure 8: Whole two-legged robot's Center of Mass (CoM) trajectory

Parameters used in previous equations take values:

$$\mathbf{A} = \begin{bmatrix} 1 & 1\cdot 10^{-3} & \frac{1}{2}\cdot 10^{-6} \\ 0 & 1 & 1\cdot 10^{-3} \\ 0 & 0 & 1 \end{bmatrix}, \qquad \mathbf{B} = \begin{bmatrix} \frac{1}{6}\cdot 10^{-9} \\ \frac{1}{2}\cdot 10^{-6} \\ 1\cdot 10^{-3} \end{bmatrix}, \qquad \mathbf{C} = [1 \quad 0 \quad 0.0372].$$

Duration of one sample is equal $T = 1$ ms, while N_L is equal:

$$N_L = 700. \tag{36}$$

N_L is the number of samples that are defining the prediction horizon (how far we are looking in the future).

This means that preview horizon is equal:

$$N_L \cdot T = 700 \cdot 1 \text{ ms} = 0.7 \text{ s}. \tag{37}$$

This length of preview horizon is high enough to detect in time sudden changes in desired ZMP trajectory and move CoM of the robot in order to follow them. Values of selected matrices:

$$\widetilde{\mathbf{A}} = \begin{bmatrix} 1 & 1 & 0.001 & -0.0255 \\ 0 & 1 & 0.001 & 0.5\cdot 10^{-6} \\ 0 & 0 & 1 & 0.001 \\ 0 & 0 & 0 & 1 \end{bmatrix}, \tag{38}$$

$$\widetilde{\mathbf{K}} \approx \begin{bmatrix} 3.6 & 653.1 & 105.7 & 0.1 \\ 653.1 & 130750.8 & 21397.1 & 44.5 \\ 105.7 & 21397.1 & 3535.6 & 7.9 \\ 0.1 & 44.5 & 7.9 & 0.1 \end{bmatrix}, \tag{39}$$

$$\widetilde{\mathbf{A}}_c \approx \begin{bmatrix} 1 & 1.9 & 0.16 & -0.02 \\ -1.6e-08 & 1 & 0.001 & 4.8e-07 \\ -4.6e-05 & -0.01 & 1 & 0.001 \\ -0.1 & -33.8 & -6.1 & 0.8 \end{bmatrix}, \tag{40}$$

$$Q_e = 0.01, \tag{41}$$

$$\mathbf{Q}_x = \begin{bmatrix} 0.01 & 0 & 0 \\ 0 & 0.001 & 0 \\ 0 & 0 & 0.001 \end{bmatrix}, \tag{42}$$

$$R = 10^{-6}. \tag{43}$$

Parameters $\widetilde{G}_i$ and $\widetilde{\mathbf{G}}_x$ are calculated according to the formulas (22), (23):

$$\widetilde{G}_i \approx 93.513, \tag{44}$$

$$\widetilde{\mathbf{G}}_x \approx [33845.908 \quad 6141.958 \quad 128.591]. \tag{45}$$

Finally, parameter $\mathbf{G}_p$ (Eq. (8)) as $N_L \times 1$ size vector is obtained (Fig. 9).

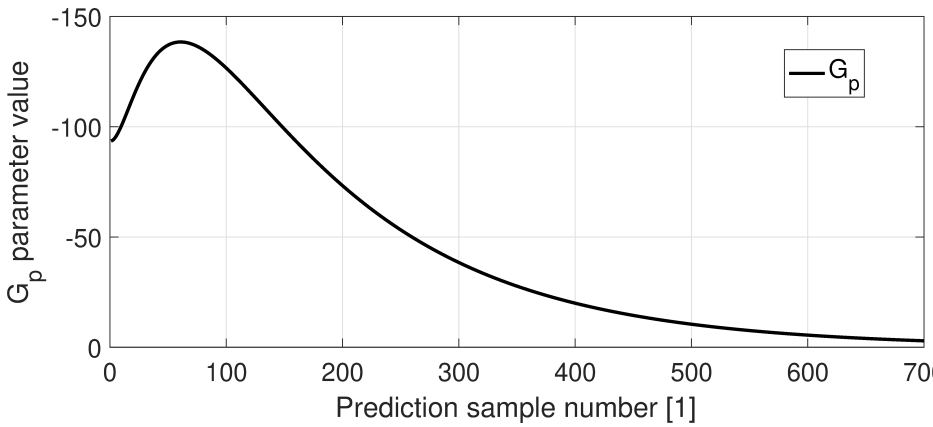

Figure 9: Generated values of G_p

5.4. Inverse kinematics problem (stage 4)

Stage 4 provides us with trajectories that should be used by humanoid robot's actuators. Fig. 10 presents the results obtained from inverse kinematics problem solution for the task defined in stage 1 – the gait parameters defined in Table 1 and robot's model described by the kinematic structure illustrated in Fig. 1, with dimensions given in Table 2.

Trajectory of Zero Moment Point (with information about the trajectory of the centre of mass of the entire system) together with trajectories of characteristic points are enough to solve inverse kinematic problem for overall robot structure. Obtained angular trajectories for all active degrees of freedom are shown in Fig. 10. For clarity, only the trajectories for left lower limb are displayed. Trajectories for the right leg are the same, but shifted in time.

As one can see, the trajectories are smooth. Maximum angles are within joint limits (as well as joint velocities and joint accelerations). Therefore the obtained trajectories can be safely implemented and verified using the real robot.

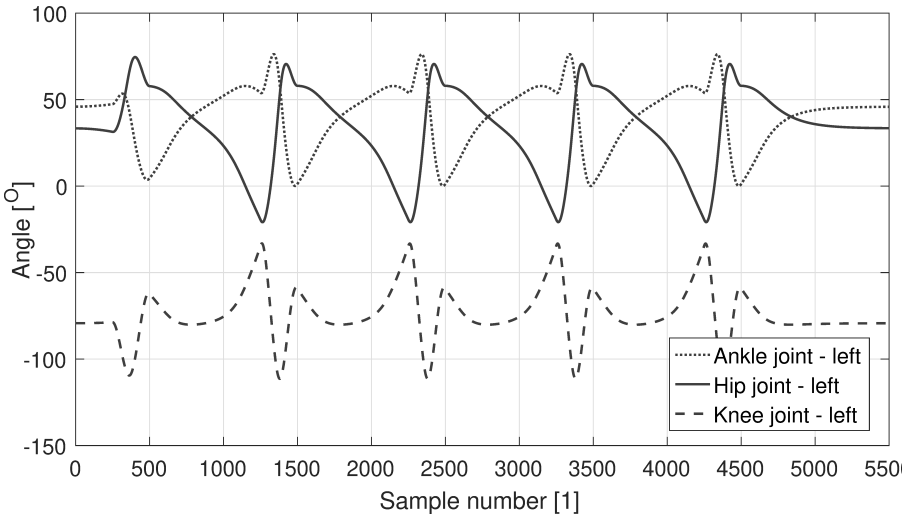

Figure 10: Joint angles trajectories for left lower limb

6. Robotic hardware – implementation

6.1. Test-bed description

Test bed consists of two components: humanoid robot and motion stabilizer. The test bed is presented in Fig. 11.

The humanoid robot in our test bed is a planar robot, which cannot move sideways, such restriction was imposed by placing the robot on a specially designed movement stabilizer. Stabilizer restricts sideways motion while allowing only the movement in the sagittal plane (front and back) is not restricted (robot can fall over). The designed restriction allowing the robot motion only in the sagittal plane eliminates the side balancing (side balancing was the subject of our previous works [7]).

The motion stabilizer is composed of two linear rails (2 meters length each), gantry and two connectors (30 cm length each; connectors' masses are small comparing to the gantry, therefore they are not present in the modelled part – we assume that they are weightless). In the revolute joints the Dynamixel MX-28 servos are used. Gantry (the moving part) is composed of the set of bearings, mechanical components stiffening the structure, robot's power supply and electronics. The mass of above mentioned gantry with instrumentation is big enough to be included in the model.

Some of the real robot construction elements were made using 3D printing technology. It allowed to obtain the elements of complex shapes, which allowed a large ranges of motion with the possibly smallest partial masses.

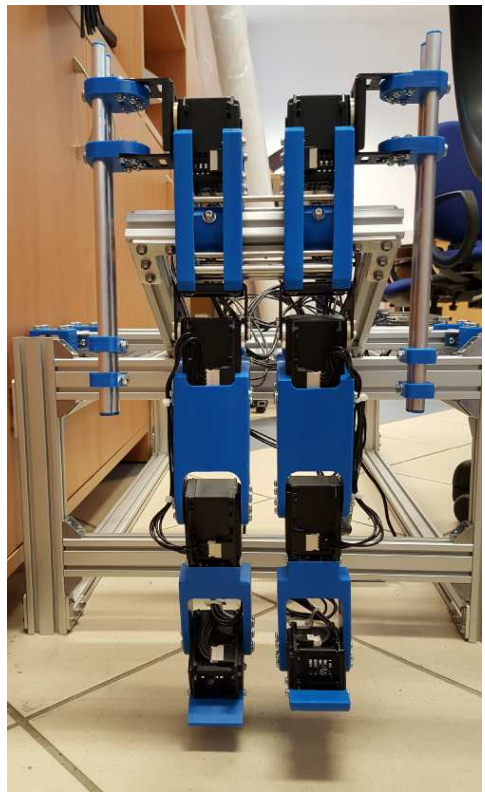

Figure 11: Humanoid robot on the stabilizer – test bed

The lengths of the robot's segments have been chosen in such way that they reflect the lengths of the segments of an adult person (in proportion to the height, according to [18]). Segments' lengths are the same as those presented in Table 2.

6.2. Results

Fig. 12 presents 5 walking cycles completed by the robot. Whole movie is available at: https://youtu.be/YZ9Y5PQZ1-4. At the beginning, the robot stands with feet parallel to each other. Movement starts with the left lower limb and ends with the right lower limb so the postures at the beginning and at the end are the same. Due to the view obstruction caused by the motion stabilizer, only the movement of left lower limb is fully visible, while the movement of the right lower limb is slightly obscured (the movement of the right leg is analogical, but shifted in time – robots steps are equal). A bright horizontal beam visible in the middle of each picture is part of slider.

The robot walked a defined number of steps without losing its balance. This confirmed the correctness of proposed algorithm.

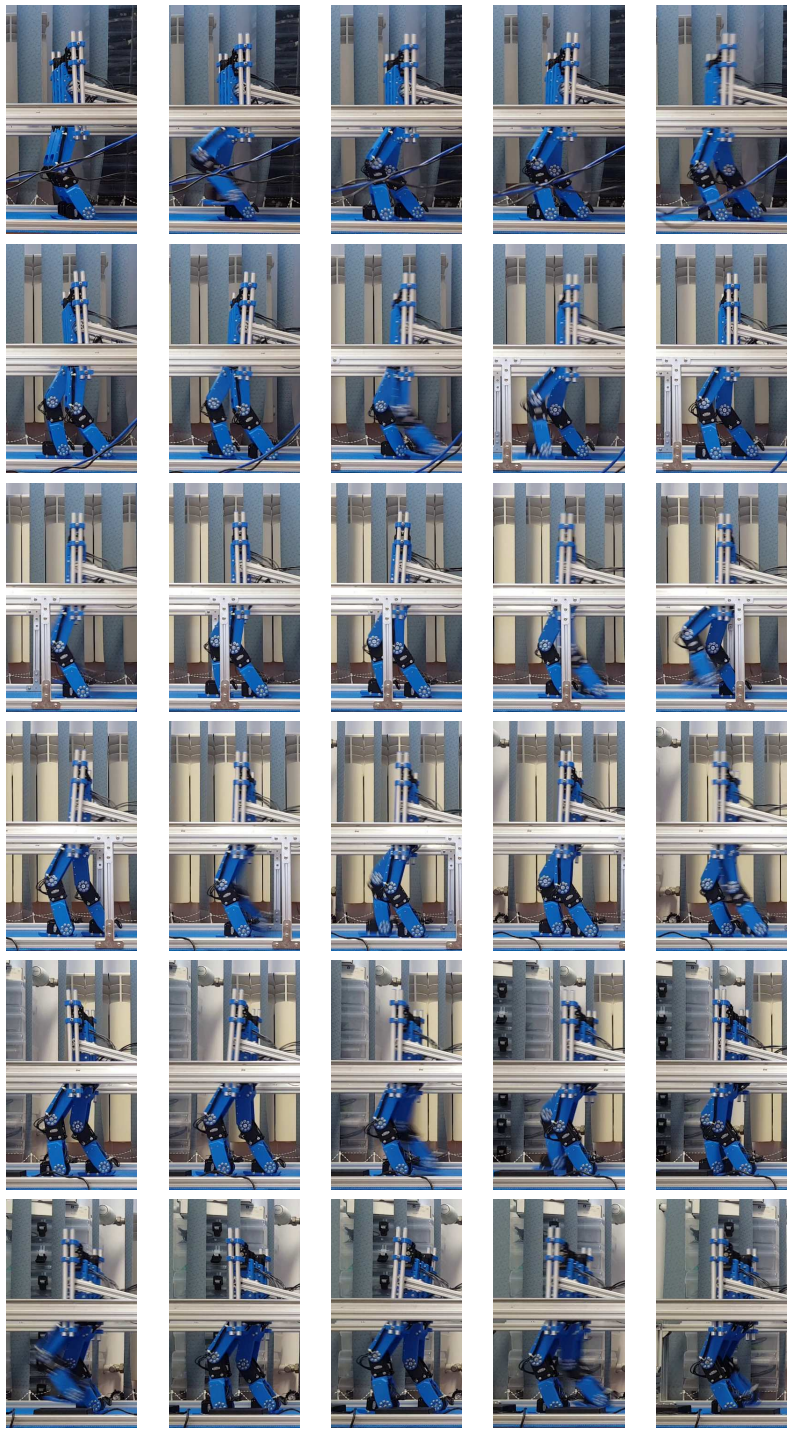

Figure 12: Gait record

7. Conclusions

This paper presents a concept of humanoid robot motion generation using the dynamic model of the robot developed by the authors – Extended Cart-Table model. Comparing to the models available in the literature ([3]), our model takes into account the motion stabilizer which is the integral part of the test bed. Algorithm presented in this paper provides us with the angular trajectories, that can be directly implemented on the real humanoid robot. Generated angular trajectories were preliminary verified and next successfully implemented in the robot. Tests performed using the real robot confirmed the correctness of the method – the robot completed a set of steps without losing its balance.

During the derivation of the method presented in this paper, some simplifications were done. The movement was generated only in sagittal plane. This simplification was done to reduce the complexity of gait generation problem (e.g. the issue of side balancing doesn't have to be considered). Also, moments of inertias in the robot model weren't considered. This resulted in easier derivation of the Zero Moment Point and having the linear model. Results presented in this paper show that those simplifications did not significantly affect the stability of the robot. Focusing on one plane only confirmed the correctness of proposed concept. Therefore the concept can be extended to next dimension, holding the same control scheme.

One of the limitations of the proposed algorithm is the simplified model. Model used in this work allows us to generate standard gait but it is not sufficient when the upper part of the body should be considered (e.g. arm movements). In the future the algorithm will be enhanced with including the motion of the upper body parts into the dynamic model (e.g. like [19]).

Further work will be also devoted to another methods of predictive control (e.g. Model Predictive Control), and models of another robots (humanoids but with different kinematic structures).

Introduction of other simplified models or other predictive control methods is not the straightforward task and lot of derivation must be done. However, in the view of the modularity of the algorithm, only one block from the control flow should be changed (the "CoM trajectory generation block" in both cases). All the rest of stages remains the same.

References

[1] C. Chevallereau, H. Razavi, D. Six, Y. Aoustin, and J. Grizzle: Self-synchronization and self-stabilization of 3D bipedal walking gaits. *Robotics and Autonomous Systems* (2018), 43–60.

[2] S.H. Collins, M. Wisse, and A. Ruina: A three-dimensional passive-dynamic walking robot with two legs and knees. *International Journal of Robotics Research*, **20**(7) (2011), 607–615.

[3] S. Kajita, F. Kanehiro, K. Kaneko, K. Fujiwara, K. Harada, K. Yokoi, and H. Hirukawa: Biped walking pattern generation by using preview control of zero-moment point. *Proc. of IEEE International Conference on Robotics and Automation* (2003), 1620–1626.

[4] S.Kajita, F. Kanehiro, K. Kaneko, K.Yokoi, and H. Hirukawa: The 3D linear inverted pendulum mode: A simple modeling for a biped walking pattern generation. *Proc. of IEEE International Conference on Intelligent Robots and Systems*, **1** (2001), 239–240.

[5] T. Katayama, T. Ohki, T. Inoue, and T. Kato: Design of an optimal controller for a discrete–time system subject to previewable demand. *Int. J. of Control*, **41** (1985), 677–699.

[6] Z. Li, N.G. Tsagarakis, and D.G Caldwell: Walking pattern generation for a humanoid robot with compliant joints. *Autonomous Robots*, **35**(1) (2016), 1–14.

[7] V. Lippi, T. Mergner, M.Szumowski, M.S. Żurawska, and T. Zielińska: Human-Inspired Humanoid Balancing and Posture Control in Frontal Plane. *Proc. of the 21st CISM-IFToMM Symposium* (2016), 285–292.

[8] Y. Liu, P.M. Wensing, D.E. Orin, and Y.F. Zheng: Dynamic walking in a humanoid robot based on a 3D Actuated Dual-SLIP model. *Proc. of IEEE Int. Conf. on Robotics and Automation* (2015), 5710–5717.

[9] R.C. Luo and C.C. Chen: Biped walking trajectory generator based on three-mass with angular momentum model using model predictive control. *IEEE Trans. on Ind. El.*, **63**(1) (2016), 268–276.

[10] K. Nishiwaki and S. Kagami: Simultaneous Planning of CoM and ZMP based on the Preview Control Method for Online Walking Control. *Proc. of 11th IEEE-RAS International Conference on Humanoid Robots*, **1**(1) (2011), 26–28.

[11] P. Parulski and K. Kozłowski: Preliminary Studies on Trajectories Generation for Walking Robot Based on Human Data. *23. International Conference on Methods and Models in Automation and Robotics MMAR*, 2018, 715–719.

[12] N. Scianca, M. Cognetti, D. De Simone, L. Lanari, and G. Oriolo: Intrinsically stable MPC for humanoid gait generation. *Proc. of IEEE-RAS 16th International Conference on Humanoid Robots* (2016), 601–606.

[13] S.E. Sovero, C.O. Saglam, and K. Byl: Passive frontal plane coupling in 3D walking. *Proc. of IEEE International Conference on Intelligent Robots and Systems* (2015), 1605–1611.

[14] K. Sreenath, H.-W. Park, I. Poulakakis, and J.W. Grizzle: A compliant hybrid zero dynamics controller for stable, efficient and fast bipedal walking on MABEL. *International Journal of Robotics Research*, **30**(9) (2011), 1170–1193.

[15] M. Szumowski, M.S. Żurawska, and T. Zielińska: ZMP Preview Control Method Application for Humanoid Robot. *Advances of Robotics* (*Postepy Robotyki*), **196** (2018), 209–218 [in Polish].

[16] P. Tatjewski: *Advanced Control of Industrial Processes, Structures and Algorithms*. Springer, 2007.

[17] M. Vukobratovic and B. Borovac: Zero Moment Point – Thirty Five Years of Its Life. *Int. Journal of Humanoid Robotics*, **1**(1) (2004), 157–173.

[18] D.A. Winter: *Biomechanics and Motor Control of Human Movement*. 4th Edition. Wiley, 2009.

[19] M.S. Żurawska, M. Szumowski, and T. Zielińska: Reconfigurable Double Inverted Pendulum Applied to the Modelling of Human Robot Motion. Journal of Automation, Mobile Robotics & Intelligent Systems, **11**(2) (2017), 12–20.

[20] "RoboCupSoccer" league description: https://www.robocup.org/domains/1, access date: 28.02.2019.